Heterogeneity in the processing of ClC-5 mutants related to Dent disease

Teddy Grand, Sébastien L'Hoste, David Mordasini, Nadia Defontaine, Mathilde Keck, Thomas Pennaforte, Mathieu Genete, Kamel Laghmani, Jacques Teulon, Stéphane Lourdel

Human Mutation

Heterogeneity in the processing of ClC-5 mutants related to Dent disease

Journal:	*Human Mutation*
Manuscript ID:	humu-2010-0263.R1
Wiley - Manuscript type:	Research Article
Date Submitted by the Author:	04-Jan-2011
Complete List of Authors:	Grand, Teddy; UPMC Univ Paris 06, UMR_S 872; INSERM, UMR_S 872; CNRS, ERL 7226 L'Hoste, Sébastien; UPMC Univ Paris 06, UMR_S 872; INSERM, UMR_S 872; CNRS, ERL 7226 Mordasini, David; UPMC Univ Paris 06, UMR_S 872; INSERM, UMR_S 872; CNRS, ERL 7226 Defontaine, Nadia; UPMC Univ Paris 06, UMR_S 872; INSERM, UMR_S 872; CNRS, ERL 7226 Keck, Mathilde; UPMC Univ Paris 06, UMR_S 872; INSERM, UMR_S 872; CNRS, ERL 7226 Pennaforte, Thomas; UPMC Univ Paris 06, UMR_S 872; INSERM, UMR_S 872; CNRS, ERL 7226 Genete, Mathieu; UPMC Univ Paris 06, UMR_S 872; INSERM, UMR_S 872; CNRS, ERL 7226 Laghmani, Kamel; UPMC Univ Paris 06, UMR_S 872; INSERM, UMR_S 872; CNRS, ERL 7226 Teulon, Jacques; UPMC Univ Paris 06, UMR_S 872; INSERM, UMR_S 872; CNRS, ERL 7226 Lourdel, Stéphane; UPMC Univ Paris 06, UMR_S 872; INSERM, UMR_S 872; CNRS, ERL 7226
Key Words:	Dent's disease, Chloride/proton exchanger, CLCN5, ClC-5, Processing

Heterogeneity in the processing of ClC-5 mutants related to Dent disease

Teddy Grand[1,2,3], Sébastien L'Hoste[1,2,3], David Mordasini[1,2,3], Nadia Defontaine[1,2,3], Mathilde Keck[1,2,3], Thomas Pennaforte[1,2,3], Mathieu Genete[1,2,3], Kamel Laghmani[1,2,3], Jacques Teulon[1,2,3] and Stéphane Lourdel[1,2,3].

[1]UPMC Univ Paris 06, UMR_S 872, Laboratoire de génomique, physiologie et physiopathologie rénales, F-75005, Paris, France

[2]INSERM, UMR_S 872, Laboratoire de génomique, physiologie et physiopathologie rénales, F-75005, Paris, France

[3]CNRS, ERL 7226, Laboratoire de génomique, physiologie et physiopathologie rénales, F-75005, Paris, France

Address for correspondence:

Stéphane Lourdel, UMR_S 872, ERL 7226, Laboratoire de génomique, physiologie et physiopathologie rénales, 15 rue de l'Ecole de Médecine, 75270 Paris cedex 06, France

phone: 33.1.55.42.78.55

fax: 33.1.46.33.41.72

e-mail: stephane.lourdel@upmc.fr

ABSTRACT

Mutations in the electrogenic Cl^-/H^+ exchanger ClC-5 gene *CLCN5* are frequently associated with Dent disease, an X-linked recessive disorder affecting the proximal tubules. Here, we investigate the consequences in *X. laevis* oocytes and in HEK293 cells of 9 previously reported, pathogenic, missense mutations of ClC-5, most of them which are located in regions forming the subunit interface. Two mutants trafficked normally to the cell surface and to early endosomes, and displayed complex glycosylation at the cell surface like wild-type ClC-5, but exhibited reduced currents. Three mutants displayed improper N-glycosylation, and were non-functional due to being retained and degraded at the endoplasmic reticulum. Functional characterization of four mutants allowed us to identify a novel mechanism leading to ClC-5 dysfunction in Dent disease. We report that these mutant proteins were delayed in their processing and that the stability of their complex glycosylated form was reduced, causing lower cell surface expression. The early endosome distribution of these mutants was normal. Half of these mutants displayed reduced currents, whereas the other half showed abolished currents. Our study revealed distinct cellular mechanisms accounting for ClC-5 loss-of-function in Dent disease.

KEY WORDS

Dent disease; Chloride/proton exchanger; *CLCN5*; ClC-5; processing.

INTRODUCTION

Dent disease is an X-linked recessive renal tubular disorder characterized by low-molecular-weight proteinuria (LMWP), hypercalciuria, nephrocalcinosis, and progressive renal failure. Inactivating mutations of *CLCN5* cause Dent disease (MIM# 300009). However, defects in *OCRL1*, the gene encoding a phosphatidylinositol-4,5-bisphosphate-5-phosphatase, have also been found in a subset of patients with Dent disease (MIM# 300555) [Hoopes, et al., 2005; Ludwig, et al., 2006].

CLCN5 encodes the electrogenic Cl^-/H^+ exchanger ClC-5 [Picollo and Pusch, 2005; Scheel, et al., 2005]. In the kidney, ClC-5 expression has been observed in the proximal tubule, in the α- and β-intercalated cells of the collecting duct, and at lower levels in the thick ascending limb of Henle's loop [Devuyst, et al., 1999; Gunther, et al., 1998]. Because ClC-5 colocalizes with v-type H^+-ATPase in renal proximal tubular subapical endosomes, the central hypothesis advanced to explain the endocytosis defect in Dent disease is that ClC-5 may provide shunt conductance in early endosomes thus permitting intraluminal acidification by v-type H^+-ATPase, and that loss-of-function of ClC-5 would therefore impair endosomal acidification, a crucial step in normal endosomal function [Devuyst, et al., 1999; Dowland, et al., 2000; Gunther, et al., 1998; Piwon, et al., 2000; Sakamoto, et al., 1999; Suzuki, et al., 2006]. However, recently, Jentsch's group has provided evidence that modulation of the chloride concentration during proton transport by the exchanger activity of ClC-5 plays a crucial role in endocytosis, rather than endosomal acidification [Novarino, et al., 2010]. A small fraction of ClC-5 is also present at the apical surface of proximal tubule cells where it may play a crucial role in mediating the protein-protein interactions required for receptor-mediated endocytosis [Wang, et al., 2005]. ClC-5 has indeed been found to associate with cofilin, a protein involved in the depolymerization of actin in the vicinity of endosomes, with

the PDZ-domain protein NHERF2, and with KIF3B, a member of the kinesin superfamily [Hryciw, et al., 2003; Reed, et al., 2010]. It has also been shown to interact in heterologous expression systems with the ubiquitin protein ligases WWP2 and Nedd4-2, which by ubiquitinating ClC-5 at his PY-motif leads to its internalization by endocytosis [Hryciw, et al., 2006a; Hryciw, et al., 2004; Schwake, et al., 2001]. However, the recent work of Rickheit *et al*. on different mouse models demonstrated that *in vivo* the PY-motif-dependent ubiquitylation of ClC-5 is not required for proximal tubular endocytosis [Rickheit, et al., 2010].

Recent studies of the functional consequences of naturally-occurring *CLCN5* mutations revealed that several different mechanisms underlie the ClC-5 loss-of-function in patients with Dent disease [Grand, et al., 2009; Ludwig, et al., 2005; Smith, et al., 2009]. On the basis of functional data, mutations were classified into different groups in previous studies by us and others [Grand, et al., 2009; Smith, et al., 2009]. A first group of mutations lead to endoplasmic reticulum retention, and degradation of the mutant proteins as they are misfolded. These amino acid substitutions were all located in helices forming the interface between the two subunits [Smith, et al., 2009]. Very similarly, we demonstrated that mutations located along α-helices at quite some distance from the interface were also trapped in the endoplasmic reticulum [Grand, et al., 2009]. These mutations were associated with reduced protein expression and impaired N-glycosylation. A second group of mutations lead to ClC-5 proteins that are devoid of electrical activity and fail to enhance endosomal acidification [Smith, et al., 2009]. A third group of mutations are associated with reduction of currents at the cell surface, reduction of plasma membrane expression and alterations in endosomal targeting [Smith, et al., 2009]. These mutant proteins were nevertheless able to support endosomal acidification. Finally, we described another type of mutations that caused

reduced currents. The mutant proteins trafficked normally to the cell surface and to early endosomes, and displayed complex glycosylation at the cell surface [Grand, et al., 2009].

These data do not rule out the possibility that other mechanisms may also contribute to the disease, because the functional aspects of numerous *CLCN5* mutations have not yet been fully investigated. We therefore decided to investigate the functional consequences of nine previously-reported ClC-5 missense mutations, by focusing on amino acid substitutions, most of which are clustered at the interface between the two subunits or at the periphery of the subunit interface.

MATERIALS AND METHODS

Molecular Biology

ClC-5 mutants (Table 1) were synthesized from human wild-type ClC-5 (GenBank NG_007159.2) extracellularly HA tagged, and subcloned into the pTLN expression vector (a generous gift of Pr. T. J. Jentsch, MDC/FMP, Berlin, Germany) for expression in *X. laevis* oocytes, or into the peGFP expression vector for expression in HEK293 cells. The HA epitope (YPYDVPDYA) is introduced into the extracellular loop of ClC-5 between transmembrane domains B and C [Dutzler, et al., 2002]. Experimental studies have shown that the HA epitope does not interfere with ClC-5 function [Schwake, et al., 2001]. Site-directed mutagenesis was performed with the Quickchange site-directed mutagenesis kit (Stratagene, La Jolla, CA, USA). All constructs were fully sequenced.

Expression in *Xenopus laevis* oocytes

Capped cRNA were synthesized *in vitro* from wild-type and mutant ClC-5 expression vectors linearized with MluI using the SP6 mMessage mMachine Kit (Ambion, Austin, TX, USA). Defolliculated *Xenopus leavis* oocytes were injected with 20 ng of the different cRNAs. The oocytes were then kept at 17°C in modified Barth's solution containing (in mM): 88 NaCl, 1 KCl, 0.41 $CaCl_2$, 0.32 $Ca(NO_3)_2$, 0.82 $MgSO_4$, 10 HEPES, pH 7.4 and gentamycin (20 µg/ml).

Electrophysiology

Five days after injection, two-electrode voltage-clamp experiments were performed at room temperature using a TEV-200A amplifier (Dagan, Minneapolis, MN, USA) and PClamp 8 software (Axon Instruments, Union City, CA, USA). Pipettes were pulled from borosilicate

glass (Harvard Apparatus, Edenbridge, Kent, UK) using a puller (Sutter Instrument Co., Novato, CA, USA), and filled with 3 M KCl. Pipette resistances were less than 1 MΩ. Currents were recorded in ND96 solution containing (in mM): 96 NaCl, 2 KCl, 1.5 $CaCl_2$, 1 $MgCl_2$, 5 HEPES, pH 7.4. Currents were recorded in response to a voltage protocol consisting of 20 mV steps from –100 mV to +100 mV during 800 ms from a holding potential of –30 mV.

Surface labelling of oocytes

Experiments were essentially performed according to the method of Zerangue *et al.* with slight modifications [Zerangue, et al., 1999]. Oocytes were incubated for 30 minutes in ND96 with 1% Bovine Serum Albumin (BSA) at 4°C to block unspecific binding, and were then incubated for 60 minutes with a rat monoclonal anti-HA antibody (1 µg/ml, 3F10, Roche Diagnostics, Meyland, France) in 1% BSA/ND96 at 4°C. The oocytes were then washed eight times with 1% BSA/ND96 at 4°C, before being incubated for 45 minutes with a peroxidase-conjugated affinity-purified F(ab')2 fragment goat anti-rat antibody (2 µg/ml, Jackson ImmunoResearch, West Grove, PA, USA) in 1% BSA/ND96 at 4°C. The oocytes were washed six times with 1% BSA/ND96 at 4°C, and then six times in ND96 without BSA at 4°C. Individual oocytes were placed in 50 µl of SuperSignal Elisa Femto Maximum Sensitivity Substrate Solution (Pierce, Rockford, IL, USA) and, after an equilibration period of 1 minute, chemiluminescence was quantified in a Turner TD-20/20 luminometer (Turner Designs, Sunnyvale, CA, USA) by integrating the signal over a period of 10 seconds.

Cell culture and transfection

HEK293 cells were grown in Dulbecco's modified Eagle's medium (DMEM) (GIBCO, Invitrogen, CA, USA) supplemented with 10% fetal bovine serum, penicillin (100 IU/ml), and streptomycin (100 µg/ml) at 37°C in 5% CO_2. The cells were transiently transfected using Fugene 6 according to the Manufacturer's instructions (Roche Diagnostics, Meyland, France).

Immunocytochemistry

Transfected HEK293 cells were plated on 12-mm diameter Petri dishes. Cells were then fixed in 4% paraformaldehyde, and permeabilized with 0.3% Triton. Nonspecific binding sites were blocked with 16% goat serum solution. The primary antibodies used were mouse anti-HA (Sigma, St Louis, MO, USA), rabbit anti-EEA1 (Sigma, St Quentin Fallavier, France), rabbit anti-calnexin (Stressgen, Ann Arbor, MI, USA). FITC-conjugated goat anti-mouse (Jackson ImmunoResearch, West Grove, PA, USA), TRITC-conjugated goat anti-rabbit (Jackson ImmunoResearch, West Grove, PA, USA), or Cy5-conjugated streptavidin (Sigma, St Quentin Fallavier, France) were added to the cells as secondary antibodies. Labeled cells were analyzed with a Zeiss LSM 510 confocal laser scanning microscope. Image analysis was performed by using ImageJ and Photoshop CS2 (Adobe, San Jose, CA, USA).

Surface biotinylation of HEK293 cells

Forty-eight hours after transfection, cells were placed on ice and rinsed twice with a cold rinsing solution containing PBS, 100 µM $CaCl_2$ and 1 mM $MgCl_2$. The cells were then incubated at 4°C for 1 h with PBS and 1.5 mg/ml NHS-biotin (Pierce, Rockford, IL, USA). They were incubated in quenching solution containing 0.1% BSA diluted in PBS, and rinsed 3

times with the rinsing solution. After lysis in a solution containing 20 mM Tris HCl, 2 mM EDTA, 2 mM EGTA, 30 mM NaF, 30 mM NaPPi, 1% Triton, 0.1% SDS and a protease inhibitor mix (Complete, Roche Diagnostics, France), equal amounts of proteins were precipitated at 4°C overnight using streptavidin-agarose beads (Pierce, Rockford, IL, USA). Samples were then centrifuged at 2,500 x g for 2 min at 4°C with TLB solution containing 50 mM Tris-HCl, pH 7.4, 100 mM NaCl, 5 mM EDTA and the protease inhibitor mix.

Protein isolation

For the isolation of total cell lysates from HEK293, the cells were incubated for 10 min on ice with the lysis solution. Samples were centrifuged at 13,000 rpm for 5 minutes. The protein concentration in the supernatant was quantified using a protein assay quantification kit (BCA Protein Kit Assay, Pierce, Rockfort, IL, USA).

Western blot analysis

The proteins were separated on an 8% SDS-PAGE gel and transferred to PVDF membranes. Primary rat anti-HA monoclonal antibody (3F10, Roche Diagnostics, Meyland, France), rabbit anti-GAPDH monoclonal antibody (Abcam, Cambridge, UK), and secondary peroxidase-conjugated goat anti-rat antibody (Jackson ImmunoResearch, West Grove, PA, USA) were diluted in TBS-blocking solution. Detection was performed using the ECL Western Blotting Substrate (Pierce, Rockford, IL, USA).

Pulse-chase assays

Prior to the experiment, HEK 293 cells were transiently transfected with plasmid DNA using Fugene 6 reagent as described above. 24 h later they were incubated in cysteine- and methionine-free DMEM starvation media for 1 h. The starvation medium was removed and

replaced with DMEM labeling medium containing [^{35}S]methionine/cysteine labeling mix. Cells were then rinsed three times with PBS, and another three times with normal growth medium before being returned to normal growth medium for the duration of the chase to the specified time points. Cells were washed twice with ice-cold PBS, and incubated on ice for 1 h in lysis buffer with a mixture of protease inhibitors, after which solubilized extracts were collected for immunoprecipitation. Proteins were immunoprecipitated with mouse anti-HA antibody (Sigma, St Louis, MO, USA), resolved with SDS-PAGE, blotted onto nitrocellulose, and revealed by autoradiography.

Statistics

Results are shown as mean ± SEM. *n* indicates the number of experiments. Statistical significance was analyzed by applying a paired Student's t-test using SigmaStat software (SPSS, Erkrath, Germany). $P < 0.05$ was considered significant.

RESULTS

We first examined the electrophysiological properties of wild-type (WT) and ClC-5 mutants by expressing them in *X. laevis* oocytes. WT ClC-5 displayed strongly outwardly-rectifying currents, as previously reported (Fig. 1A and B) [Friedrich, et al., 1999; Grand, et al., 2009; Picollo and Pusch, 2005; Scheel, et al., 2005; Smith, et al., 2009; Steinmeyer, et al., 1995]. Compared to oocytes injected with WT ClC-5, oocytes expressing the W547G mutant (c.1714T>G; p.W547G) displayed a significant reduction by 67% (n = 28) in current amplitude (Fig. 1A and 2). The S244L (c.806C>T; p.S244L) and L278F (c.910G>C; p.L278F) mutants showed current reductions of 75% (n = 13) and 63% (n = 6) respectively, which was consistent with previous reports (Fig. 1 and 2) [Igarashi, et al., 1998; Lloyd, et al., 1996; Lloyd, et al., 1997; Smith, et al., 2009]. Despite this reduced current amplitude, the voltage dependence of the currents with these mutants resembled those of WT ClC-5 (Fig. 1). In contrast, currents in oocytes injected with the L225P (c.750T>C; p.L225P) (n = 11), G260V (c.855G>T; p.G260V) (n = 8), Y272C (c.891A>G; p.Y272C) (n = 8), N340K (c.1096C>A; p.N340K) (n = 21), G513R (c.1612G>C; p.G513R) (n = 7), and K546E (c.1712A>G; p.K546E) mutants (n = 6) were not significantly different from those observed in non-injected oocytes (Fig. 1 and 2).

We and other authors have previously shown that several *CLCN5* missense mutations reduce or abolish ClC-5 currents at the plasma membrane as a result of reduced trafficking of the protein to the cell surface or to enhanced endoplasmic reticulum retention and the resulting increased protein degradation [Grand, et al., 2009; Ludwig, et al., 2005; Smith, et al., 2009]. To further elucidate the mechanisms leading to altered currents, we next investigated the cell surface targeting of WT and mutant ClC-5 proteins in *X. leavis* oocytes. Levels of the S244L and Y272C mutants in the plasma membrane were comparable (Fig. 2). Thus, the

significant decrease in current amplitudes in the S244L mutant, and the loss of electrical activity in the Y272C mutant (Fig. 1A and B, Fig. 2) cannot be ascribed to reduced protein trafficking to the cell surface. In contrast, the G260V, L278F, K546E, and W547G mutants all showed reductions of 25-50% in their surface expression, and no surface expression at all was detected with the L225P, N340K, and G513R mutants. The change in electrical activity observed with these latter ClC-5 mutants could be explained by the abolition or impairment of cell-surface expression due to mis-targeting (Fig. 1A and B, Fig. 2) or altered protein expression.

To check their protein expression, total cell lysates isolated from HEK293 cells transiently transfected with either WT or mutant ClC-5 were subjected to a western blot analysis (Fig. 3). In our previous study, we reported positive western blot staining for the 90-kDa core-glycosylated and the 100-kDa complex glycosylated forms of WT ClC-5 [Grand, et al., 2009]. We also showed that the 90-kDa ClC-5 protein displays high mannose glycosylation, and is retained in the endoplasmic reticulum, and that the plasma membrane ClC-5 component displays complex glycosylation [Grand, et al., 2009]. Here, when an equivalent amount of proteins was loaded in each lane, no significant difference in density or size could be detected between WT ClC-5 and the S244L and Y272C mutants. In contrast, the 100-kDa complex glycosylated form/90-kDa core-glycosylated form ratio was significantly reduced by ~50% for the G260V, L278F, K546E and W547G mutants versus WT ClC-5. Thus, the decreased currents in the S244L and Y272C mutants were not attributable to differing levels of protein expression. However, the altered currents in the L278F, G260V, K546E and W547E mutants could be attributable to reduced amounts of the complex glycosylated component, which could result from changes in the post-translational processing or from an increase in the turnover of the mutant proteins (Fig. 3). In contrast, only the 90-kDa core-glycosylated form of ClC-5 was detected in the L225P, N340K, and G513R mutants

(Fig. 3). The abolition of conduction and surface expression in these latter mutants can be the consequence of a rapid degradation of the proteins within the cell. These results are similar to what we had previously reported for other ClC-5 mutants [Grand, et al., 2009].

We then compared the stability and the maturation of one out of the four similar mutants showing a reduction of ~50% of the 100-kDa complex glycosylated form/90-kDa core-glycosylated form of ClC-5 (G260V, Fig. 3) and one out of the three similar mutants showing only the 90-kDa core-glycosylated form of ClC-5 (L225P, Fig. 3) with those of WT ClC-5, by tracing the sorting and delivery of newly synthesized proteins from the endoplasmic reticulum to Golgi compartments by means of a pulse-chase analysis. We observed that the WT ClC-5 protein migrated as the 90-kDa core-glycosylated form immediately after pulse labeling (Fig. 4A). The 100-kDa complex glycosylated form, which was barely visible at the end of the pulse period, increased in amount during the first hour of chase, and became the predominant form by 2 hours (Fig. 4A). Kinetic analysis (Fig. 4B-C) revealed a progressive decrease in the 90-kDa immature form of the WT ClC-5 protein, with half-life of 1.5 hours (n = 3), and a progressive increase in the 100-kDa mature form of the WT ClC-5 protein (n = 3). The decrease represents the conversion of the immature form to the mature form as well as the degradation of the immature form of ClC-5 protein. Likewise, the G260V mutant protein was initially converted from the core-glycosylated form to the complex glycosylated form, like WT ClC-5 (Fig. 4A). The degradation of the immature form of WT ClC-5 and the G260V mutant followed the same kinetic (Fig. 4B, n = 3), but the conversion of the G260V mutant into its mature, complex glycosylated form was significantly slower than that of WT ClC-5 (Fig. 4B-C, n = 3). Furthermore, there was significant reduction between WT ClC-5 and the G260V mutant in the maximum amount of the mature form at 4 hours of chase (Fig. 4B, n = 3). In contrast to the G260V mutant, the L225P mutant was initially synthesized as the 90-kDa core-glycosylated form, but had not acquired complex

sugars at any of the time intervals, and so was not converted into the mature form during the chase (Fig. 4A). The half-life of the immature form of L225P was 50% shorter than that of WT ClC-5 (Fig. 4B, $n = 3$).

Overall, our results demonstrate that the G260V, L278F, K546E and W547G mutations lead to a delay in the maturation and to a decrease of the stability of the mature, complex glycosylated form of ClC-5, whereas the L225P, N340K and G513R mutations abolish the maturation of ClC-5.

In the light of the above findings, we next investigated the behavior of the different ClC-5 mutants at the cellular level by assessing their subcellular distribution by means of immunostaining and confocal microscopy in transiently-transfected HEK293 cells. As expected from previous reports, WT ClC-5 colocalized with biotinylated cell-surface proteins, and with the early endosomes marker EEA1 (Fig. 5) [Dowland, et al., 2000; Grand, et al., 2009; Smith, et al., 2009; Suzuki, et al., 2006]. A similar distribution was found for the Y272C and the W547G mutants (Fig. 5), and for the S244L, G260V, L278F, and K546E mutants (data not shown). In contrast to WT ClC-5, the L225P, N340K, and G513R mutants were retained in the endoplasmic reticulum compartment, as indicated by their colocalization with the endoplasmic reticulum marker calnexin, and were excluded from the plasma membrane (Fig. 5). To further explore the plasma membrane expression of the mutant ClC-5, we performed cell surface biotinylation experiments (Fig. 6). No significant difference could be detected between the surface fraction containing WT ClC-5, and that containing the S244L mutant ($n = 3$). In contrast, the abundance of the G260V mutant at the cell surface was significantly lower than that of WT ClC-5 ($n = 3$). Surface biotinylation experiments also showed that the G513R was excluded from the surface biotinylated protein fraction ($n = 3$) (Fig. 6). Overall, the endoplasmic reticulum retention of the L225P, N340K, and G513R mutants was compatible with abolition of their conduction and surface expression, which is

likely to result in rapid degradation of these proteins within the cell, as shown by our pulse-chase analysis conducted on the L225P mutant in HEK293 cells.

The functional effects of the *CLCN5* mutations we studied are summarized in Table 1.

DISCUSSION

We performed functional, biochemical, and cell-biology analyses in *X. laevis* oocytes and in HEK293 cells of nine *CLCN5* pathogenic missense mutations that had been described before [Anglani, et al., 2006; Hoopes, et al., 2004; Igarashi, et al., 1998; Lloyd, et al., 1996; Ramos-Trujillo, et al., 2007; Tosetto, et al., 2006].

The G260V, Y272C, L278F, G513R, K546E, and W547G mutations are located in helix H, in the loop between helices H and I, in helix I, and in helices O and Q, respectively (Fig. 7). Helices H, I, O and Q are involved in the formation of the dimer interface, as are helices B and P [Dutzler, et al., 2002; Dutzler, et al., 2003; Wu, et al., 2003]. Previous published modeling studies of ClC-5 based on the crystal structures of two prokaryotic ClCs suggested that ClC-5 missense mutations clustering at the dimer interface would cause a loss of electrical activity by disrupting the assembly of the homodimers [Smith, et al., 2009; Wu, et al., 2003]. This would result in the formation of misfolded proteins in the endoplasmic reticulum, and their rapid degradation within the cell. Alternatively, mutations of residues positioned in a subgroup at the periphery of the dimer interface would be associated with residual currents at the cell surface, because they would induce a relatively minor disruption of the protein structure. Our results using the L278F and the G513R mutations are consistent with these modeling studies. On the one hand, despite reduced cell surface expression, the L278F mutant exhibited residual activity and its early endosomal distribution was similar to that of WT ClC-5. It should be noted that the amino acid substitution is located in helix I at the periphery of the subunit interface. On the other hand, the G513R mutant showed no functional expression in electrophysiological recordings, and was improperly N-glycosylated due to being retained on the endoplasmic reticulum. However, in contrast to this mutant, the Y272C mutants were normally N-glycosylated, properly targeted to the plasma membrane

and to the early endosomes like WT ClC-5, and displayed reduced electrical activity. Furthermore, the G260V, K546E and W547G mutants also escaped endoplasmic reticulum retention and subsequent degradation, as shown by their complex glycosylation and plasma membrane expression. Like the L278F mutant, the cell surface expression of the mature, complex glycosylated form of these mutants was, however, reduced. Our results indicate that this may be explained by a delay in the maturation and by a decreased stability of the mature form of ClC-5. These mutant proteins were also distributed in the early endosomes. Interestingly, the reduction of currents correlated with the decreased surface expression of the mature forms for the L278F and the W547G mutants. In contrast, despite a comparable decreased level expression of their mature form at the plasma membrane like the L278F and W547G mutants, we failed to record any currents with the G260V and K546E mutants, indicating that these mutants ClC-5 displayed abolished electrical activity. Taken together, these results demonstrate that mutation of a residue located at the interface may cause less protein-folding defects than expected from previous published modeling data even though they are positioned at the interface between the two subunits [Smith, et al., 2009; Wu, et al., 2003].

The S244L mutation was shown to severely reduce currents, and was associated with unaffected trafficking to the plasma membrane and to the early endosomes, and unaltered N-glycosylation. This mutation is located in helix G (Fig. 7), a helix that is not involved in the formation of the transporter interface, or the transport pathways of Cl^- or H^+ [Chen and Hwang, 2008; Dutzler, et al., 2002; Dutzler, et al., 2003]. Further studies are required to assess the exact mechanism responsible for the reduced electrical activity of the S244L mutant.

Finally, the L225P and N340K mutants showed no functional expression in electrophysiological recordings, and were improperly N-glycosylated as a result of being

retained in the endoplasmic reticulum by quality control systems. Moreover, pulse-chase analysis of the L225P mutant demonstrated early degradation of the mutant protein. Results for these mutations, which are located in helices F and J (Fig. 7), are in accordance with our previous data and show that amino acid substitutions located within α-helices at quite some distance from the transporter interface enhance protein degradation, probably by distorting the structure of the α-helices, and preventing the proper folding of the monomer [Grand, et al., 2009]. Defects in protein folding and processing have been shown to be involved in the pathogenesis of several inherited disorders [Gregersen, et al., 2006]. One well-known example is cystic fibrosis, which is caused by mutations in the cystic fibrosis transmembrane conductance regulator (*CFTR*) gene encoding a chloride channel. Many mutant forms of the CFTR are misfolded, achieve only partial N-glycosylation, and are retained and degraded within the endoplasmic reticulum. Thus, the mechanism of transporter dysfunction identified for the type-II mutations appears to be similar to the mechanisms responsible for most cases of cystic fibrosis.

Recently, we found that two types of ClC-5 mutants can be distinguished [Grand, et al., 2009]. Here, in the line with our functional analysis, we demonstrated that five mutations (L225P, S244L, Y272C, N340K and G513R) corresponded to these two types of *CLCN5* mutations (Table 1). However, in addition, our data also revealed that four mutations (G260V, L278F, K546E and W547G) could be grouped to form a novel type of *CLCN5* mutations. These type-III mutations (Table 1) enhance a delay in the processing of ClC-5, a decrease of the stability of its mature, complex glycosylated form, a reduction of its cell surface expression, and a reduction of currents at the plasma membrane. The distribution of these mutants in the early endosomes is normal.

Another interesting aspect of our study is that 6 out of the 9 mutants were associated with expression at the cell surface in HEK293 transfected cells. Although ion conduction

through ClC-5 is thought not to be physiologically relevant at the cell surface, several recent studies in transfected proximal tubule cells have demonstrated that the ClC-5 population at the brush border is a rate-limiting step in receptor-mediated endocytosis by mediating protein-protein interactions with a variety of proteins essential for renal reabsorption [Hryciw, et al., 2006b]. In the case of the type-III mutants, one could speculate that their lower abundance at the plasma membrane could severely reduce the endocytosis by altering protein-protein interactions that are required in the formation of the endocytic macromolecular complex. The ClC-5 type-I mutants should not prevent these interactions, because they displayed normal protein expression and subcellular localization. However, these mutants displayed reduced (S244L) and abolished currents (Y272C). As a consequence, one may explain the presence of Dent disease in patients carrying these mutations by altered endosomal acidification leading to impaired receptor-mediated endocytosis, due to alteration of the function of v-type H^+-ATPase caused by reduced or abolished chloride shunt conductance. Alternatively, one may also hypothesize that chloride accumulation in early endosomes could be compromised due to decreased electrical activity of ClC-5. In the view of the recent work of Novarino *et al.*, this could also lead to altered endocytosis. Further experiments are needed to confirm these hypothesis.

Numerous *in vitro* studies have shown that dysfunctional channels or transporters can be rescued by pharmacological therapy. For example, this is the case for CFTR in patients with cystic fibrosis [Kerem, 2005]. Chemical and molecular chaperones have been shown to allow class-II CFTR mutants to escape from degradation in the endoplasmic reticulum and to be transported to the cell surface. Several compounds have also been found to directly activate class-III and class-IV CFTR mutants that display defective regulation and conduction at the plasma membrane, respectively. The findings of this study, together with previous data from the functional analysis of ClC-5 mutations in Dent disease, provide new clues for future

studies [Grand, et al., 2009; Ludwig, et al., 2005; Smith, et al., 2009]. A major challenge for such studies will be to find specific therapeutic drugs that are able to restore sufficient ClC-5 function in patients with Dent disease.

ACKNOWLEDGMENTS

This work was supported in part by grants from the French ANR program (ANR-05-MRAR-033-01), and the Bonus Qualité Recherche from the UPMC-Université Paris 06. We thank Prof. T.J. Jentsch for kindly providing the HA-tagged ClC-5, and C. Klein for excellent technical assistance in confocal microscopy. T. Grand holds a PhD fellowship from the Ministère de l'Enseignement supérieur et de la Recherche. The English text was edited by M. Ghosh.

REFERENCES

Anglani F, Bernich P, Tosetto E, Cara M, Lupo A, Nalesso F, D'Angelo A, Gambaro G. 2006. Family history may be misleading in the diagnosis of Dent's disease. Urol Res 34:61-3.

Chen TY, Hwang TC. 2008. CLC-0 and CFTR: chloride channels evolved from transporters. Physiol Rev 88:351-87.

Devuyst O, Christie PT, Courtoy PJ, Beauwens R, Thakker RV. 1999. Intra-renal and subcellular distribution of the human chloride channel, CLC-5, reveals a pathophysiological basis for Dent's disease. Hum Mol Genet 8:247-57.

Dowland LK, Luyckx VA, Enck AH, Leclercq B, Yu AS. 2000. Molecular cloning and characterization of an intracellular chloride channel in the proximal tubule cell line, LLC-PK1. J Biol Chem 275:37765-73.

Dutzler R, Campbell EB, Cadene M, Chait BT, MacKinnon R. 2002. X-ray structure of a ClC chloride channel at 3.0 A reveals the molecular basis of anion selectivity. Nature 415:287-94.

Dutzler R, Campbell EB, MacKinnon R. 2003. Gating the selectivity filter in ClC chloride channels. Science 300:108-12.

Friedrich T, Breiderhoff T, Jentsch TJ. 1999. Mutational analysis demonstrates that ClC-4 and ClC-5 directly mediate plasma membrane currents. J Biol Chem 274:896-902.

Grand T, Mordasini D, L'Hoste S, Pennaforte T, Genete M, Biyeyeme MJ, Vargas-Poussou R, Blanchard A, Teulon J, Lourdel S. 2009. Novel CLCN5 mutations in patients with Dent's disease result in altered ion currents or impaired exchanger processing. Kidney Int 76:999-1005.

Gregersen N, Bross P, Vang S, Christensen JH. 2006. Protein misfolding and human disease. Annu Rev Genomics Hum Genet 7:103-24.

Gunther W, Luchow A, Cluzeaud F, Vandewalle A, Jentsch TJ. 1998. ClC-5, the chloride channel mutated in Dent's disease, colocalizes with the proton pump in endocytotically active kidney cells. Proc Natl Acad Sci U S A 95:8075-80.

Hoopes RR, Jr., Raja KM, Koich A, Hueber P, Reid R, Knohl SJ, Scheinman SJ. 2004. Evidence for genetic heterogeneity in Dent's disease. Kidney Int 65:1615-20.

Hoopes RR, Jr., Shrimpton AE, Knohl SJ, Hueber P, Hoppe B, Matyus J, Simckes A, Tasic V, Toenshoff B, Suchy SF and others. 2005. Dent Disease with mutations in OCRL1. Am J Hum Genet 76:260-7.

Hryciw DH, Ekberg J, Ferguson C, Lee A, Wang D, Parton RG, Pollock CA, Yun CC, Poronnik P. 2006a. Regulation of albumin endocytosis by PSD95/Dlg/ZO-1 (PDZ) scaffolds. Interaction of Na^+-H^+ exchange regulatory factor-2 with ClC-5. J Biol Chem 281:16068-77.

Hryciw DH, Ekberg J, Lee A, Lensink IL, Kumar S, Guggino WB, Cook DI, Pollock CA, Poronnik P. 2004. Nedd4-2 functionally interacts with ClC-5: involvement in constitutive albumin endocytosis in proximal tubule cells. J Biol Chem 279:54996-5007.

Hryciw DH, Ekberg J, Pollock CA, Poronnik P. 2006b. ClC-5: a chloride channel with multiple roles in renal tubular albumin uptake. Int J Biochem Cell Biol 38:1036-42.

Hryciw DH, Wang Y, Devuyst O, Pollock CA, Poronnik P, Guggino WB. 2003. Cofilin interacts with ClC-5 and regulates albumin uptake in proximal tubule cell lines. J Biol Chem 278:40169-76.

Igarashi T, Gunther W, Sekine T, Inatomi J, Shiraga H, Takahashi S, Suzuki J, Tsuru N, Yanagihara T, Shimazu M and others. 1998. Functional characterization of renal chloride channel, CLCN5, mutations associated with Dent's Japan disease. Kidney Int 54:1850-6.

Kerem E. 2005. Pharmacological induction of CFTR function in patients with cystic fibrosis: mutation-specific therapy. Pediatr Pulmonol 40:183-96.

Lloyd SE, Pearce SH, Fisher SE, Steinmeyer K, Schwappach B, Scheinman SJ, Harding B, Bolino A, Devoto M, Goodyer P and others. 1996. A common molecular basis for three inherited kidney stone diseases. Nature 379:445-9.

Lloyd SE, Pearce SH, Gunther W, Kawaguchi H, Igarashi T, Jentsch TJ, Thakker RV. 1997. Idiopathic low molecular weight proteinuria associated with hypercalciuric nephrocalcinosis in Japanese children is due to mutations of the renal chloride channel (CLCN5). J Clin Invest 99:967-74.

Ludwig M, Doroszewicz J, Seyberth HW, Bokenkamp A, Balluch B, Nuutinen M, Utsch B, Waldegger S. 2005. Functional evaluation of Dent's disease-causing mutations: implications for ClC-5 channel trafficking and internalization. Hum Genet 117:228-37.

Ludwig M, Utsch B, Monnens LA. 2006. Recent advances in understanding the clinical and genetic heterogeneity of Dent's disease. Nephrol Dial Transplant 21:2708-17.

Novarino G, Weinert S, Rickheit G, Jentsch TJ. 2010. Endosomal chloride-proton exchange rather than chloride conductance is crucial for renal endocytosis. Science 328:1398-401.

Picollo A, Pusch M. 2005. Chloride/proton antiporter activity of mammalian CLC proteins ClC-4 and ClC-5. Nature 436:420-3.

Piwon N, Gunther W, Schwake M, Bosl MR, Jentsch TJ. 2000. ClC-5 Cl^- -channel disruption impairs endocytosis in a mouse model for Dent's disease. Nature 408:369-73.

Ramos-Trujillo E, Gonzalez-Acosta H, Flores C, Garcia-Nieto V, Guillen E, Gracia S, Vicente C, Espinosa L, Maseda MA, Santos F and others. 2007. A missense mutation in the chloride/proton ClC-5 antiporter gene results in increased expression of an alternative mRNA form that lacks exons 10 and 11. Identification of seven new CLCN5 mutations in patients with Dent's disease. J Hum Genet 52:255-61.

Reed AA, Loh NY, Terryn S, Lippiat JD, Partridge C, Galvanovskis J, Williams SE, Jouret F, Wu FT, Courtoy PJ and others. 2010. CLC-5 and KIF3B interact to facilitate CLC-5 plasma membrane expression, endocytosis, and microtubular transport: relevance to pathophysiology of Dent's disease. Am J Physiol Renal Physiol 298:F365-80.

Rickheit G, Wartosch L, Schaffer S, Stobrawa SM, Novarino G, Weinert S, Jentsch TJ. 2010. Role of ClC-5 in renal endocytosis is unique among ClC exchangers and does not require PY-motif-dependent ubiquitylation. J Biol Chem 285:17595-603.

Sakamoto H, Sado Y, Naito I, Kwon TH, Inoue S, Endo K, Kawasaki M, Uchida S, Nielsen S, Sasaki S and others. 1999. Cellular and subcellular immunolocalization of ClC-5 channel in mouse kidney: colocalization with H^+-ATPase. Am J Physiol 277:F957-65.

Scheel O, Zdebik AA, Lourdel S, Jentsch TJ. 2005. Voltage-dependent electrogenic chloride/proton exchange by endosomal CLC proteins. Nature 436:424-7.

Schwake M, Friedrich T, Jentsch TJ. 2001. An internalization signal in ClC-5, an endosomal Cl-channel mutated in Dent's disease. J Biol Chem 276:12049-54.

Smith AJ, Reed AA, Loh NY, Thakker RV, Lippiat JD. 2009. Characterization of Dent's disease mutations of CLC-5 reveals a correlation between functional and cell biological consequences and protein structure. Am J Physiol Renal Physiol 296:F390-7.

Steinmeyer K, Schwappach B, Bens M, Vandewalle A, Jentsch TJ. 1995. Cloning and functional expression of rat CLC-5, a chloride channel related to kidney disease. J Biol Chem 270:31172-7.

Suzuki T, Rai T, Hayama A, Sohara E, Suda S, Itoh T, Sasaki S, Uchida S. 2006. Intracellular localization of ClC chloride channels and their ability to form hetero-oligomers. J Cell Physiol 206:792-8.

Tosetto E, Ghiggeri GM, Emma F, Barbano G, Carrea A, Vezzoli G, Torregrossa R, Cara M, Ripanti G, Ammenti A and others. 2006. Phenotypic and genetic heterogeneity in Dent's disease-the results of an Italian collaborative study. Nephrol Dial Transplant 21:2452-63.

Wang Y, Cai H, Cebotaru L, Hryciw DH, Weinman EJ, Donowitz M, Guggino SE, Guggino WB. 2005. ClC-5: role in endocytosis in the proximal tubule. Am J Physiol Renal Physiol 289:F850-62.

Wu F, Roche P, Christie PT, Loh NY, Reed AA, Esnouf RM, Thakker RV. 2003. Modeling study of human renal chloride channel (hCLC-5) mutations suggests a structural-functional relationship. Kidney Int 63:1426-32.

Zerangue N, Schwappach B, Jan YN, Jan LY. 1999. A new ER trafficking signal regulates the subunit stoichiometry of plasma membrane K(ATP) channels. Neuron 22:537-48.

FIGURE LEGENDS

Figure 1. Electrophysiological characterization of WT and mutant ClC-5 in *X. laevis* oocytes. **A:** Steady-state current-voltage relationships obtained in ND96 solution (pH 7.4). Each data point represents the mean ± SEM for at least 6 oocytes from three different oocyte batches. For clarity, not all the mutants are represented. **B:** Representative original voltage-clamp recordings obtained from oocytes expressing WT ClC-5 and mutant ClC-5, and from non-injected oocytes under same conditions as described in A. WT, oocytes injected with wild-type ClC-5; NI, Non-Injected oocytes.

Figure 2. Currents/cell surface expression relationship for WT and mutants ClC-5 in *X. laevis* oocytes. Currents at +100 mV are from the same data as in Fig. 1A. For cell surface expression, the values (measured in RLU: Relative Light Units) were normalized to those of WT ClC-5 in the same batch of oocytes. Each column represents the mean ± SEM for at least 6 oocytes for current recordings, and at least 60 oocytes from three different batches of oocytes for the surface expression. *, $P < 0.001$ is the difference between WT or mutant ClC-5 vs NI. #, $P < 0.001$ is the difference between NI or mutant ClC-5 vs WT ClC-5. WT, oocytes injected with wild-type ClC-5; NI, Non-Injected oocytes.

Figure 3. Western blot analysis of total expression levels of WT and mutants ClC-5 in HEK293 transfected cells. Total cell lysates were isolated from untransfected HEK293 cells or HEK293 transfected cells. Calnexin was used as the loading marker of the samples. WT, HEK293 cells transfected with wild-type ClC-5; UT, Untransfected HEK293 cells.

Figure 4. Pulse-chase analysis of WT and mutant ClC-5 in HEK293 transfected cells. **A:** WT and mutant ClC-5 were metabolically labeled for 3 h, and chased for 0 h, 1 h, 2 h and 4 h. The ClC-5 proteins were then immunoprecipitated by anti-HA antibody, and run on SDS-PAGE gel followed by autoradiography. **B:** Quantitative analysis of immature WT and mutant ClC-5. **C:** Quantitative analysis of mature WT and mutant ClC-5. *, $P < 0.05$ is the difference between WT ClC-5 *vs* mutant ClC-5.

Figure 5. Immunocytochemical localization of WT and mutant ClC-5 in HEK293-transfected cells. ClC-5 expression was detected by green fluorescence. Organelles were stained with one of three markers: biotin (plasma membrane), EEA1 (early endosomes), calnexin (endoplasmic reticulum), and were detected by red fluorescence. The yellow fluorescence indicates that the two proteins overlap. Scale bars, 5 µm.

Figure 6. Cell surface expression of WT and mutant ClC-5 in HEK293 transfected cells. Results are shown as western blot analysis of the surface biotinylated protein fraction (S) or total cell lysates (T). UT, untransfected HEK293 cells; WT, HEK293 cells transfected with wild-type ClC-5.

Figure 7. Amino acid sequence alignment of several ClCs showing the positions of the *CLCN5* mutations characterized in this study. The conserved regions are shown in bold and highlighted in gray. Mutations are shown above the sequences. The alignment was performed using BioEdit.

Table 1. Summary of the mutations in the *CLCN5* gene studied in patients with Dent disease.

Nucleotide change[a]	Amino acid change	Position in protein structure	Currents	Surface expression	Intracellular localization		N-Glycosylation
					Endoplasmic reticulum	Early endosomes	
WT			+	+	+	+	Complex
Type-I							
c.731C>T	p.S244L	Helix G	Reduced	+	+	+	Complex
c.815A>G	p.Y272C	Loop H-I	-	+	+	+	Complex
Type-II							
c.674T>C	p.L225P	Helix F	-	-	+	-	Core
c.1020C>A	p.N340K	Helix J	-	-	+	-	Core
c.1538G>A	p.G513R	Helix O	-	-	+	-	Core
Type-III							
c.779G>T	p.G260V	Helix H	-	Reduced	+	+	Complex, reduced
c.834G>C	p.L278F	Helix I	Reduced	Reduced	+	+	Complex, reduced
c.1637A>G	p.K546E	Helix Q	-	Reduced	+	+	Complex, reduced
c.1639T>G	p.W547G	Helix Q	Reduced	Reduced	+	+	Complex, reduced

[a]Nucleotide numbering refers to the cDNA numbering with +1 being the A of the ATG translation initiation codon in the reference sequence, according to journal guidelines (www.hgvs.org/mutnomen). Codon 1 is the initiation codon. Human wild-type ClC-5 GenBank assession number is NG_007159.2.

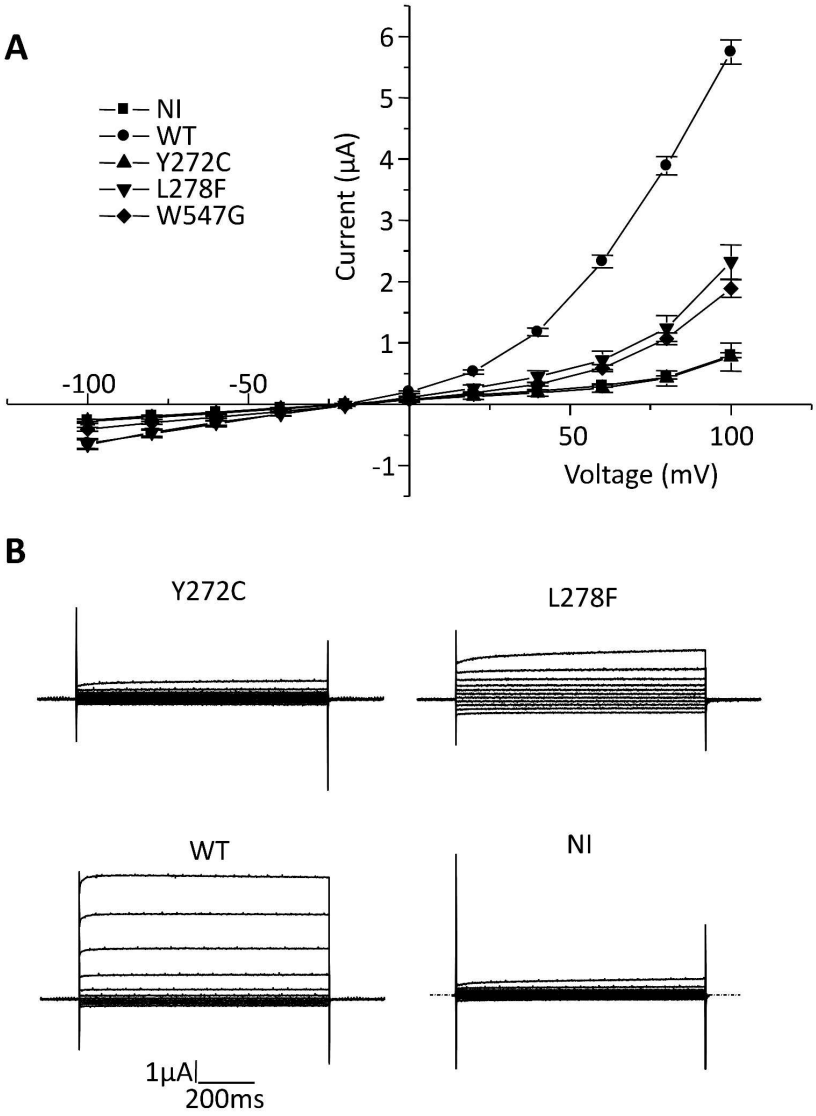

Figure 1

261x378mm (300 x 300 DPI)

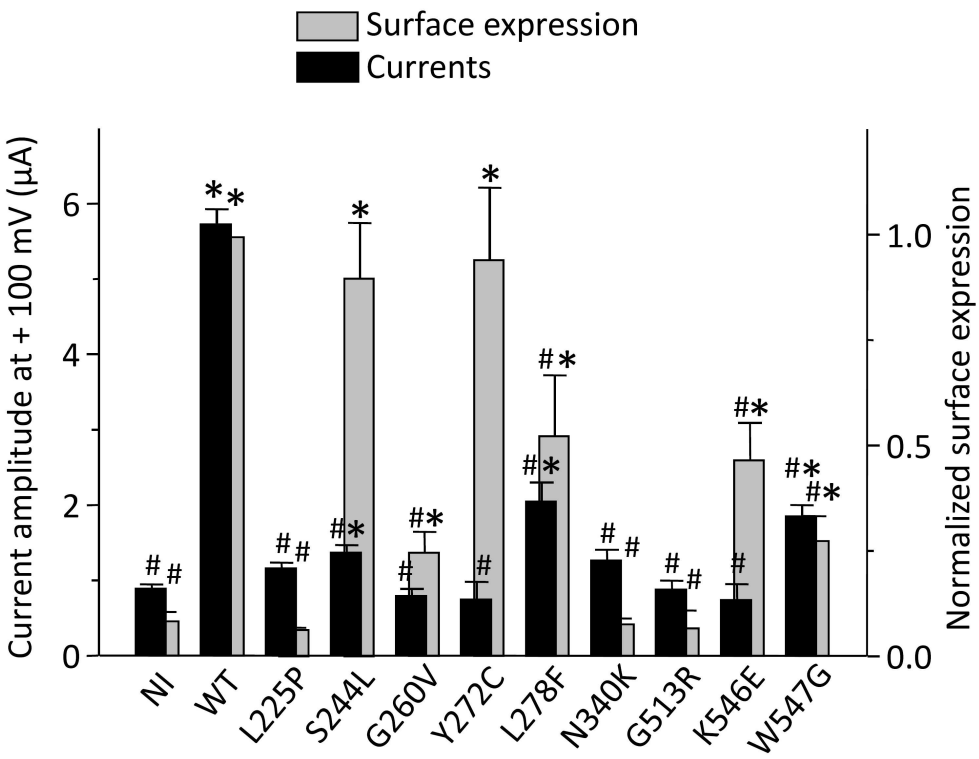

Figure 2

258x219mm (300 x 300 DPI)

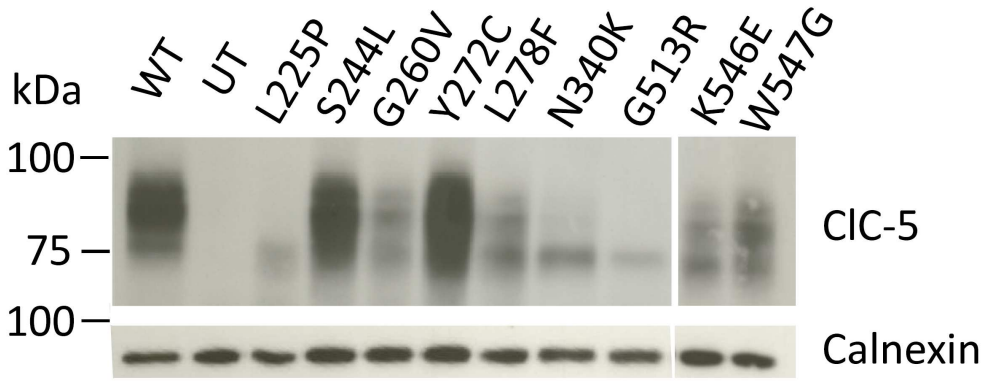

Figure 3

200x109mm (300 x 300 DPI)

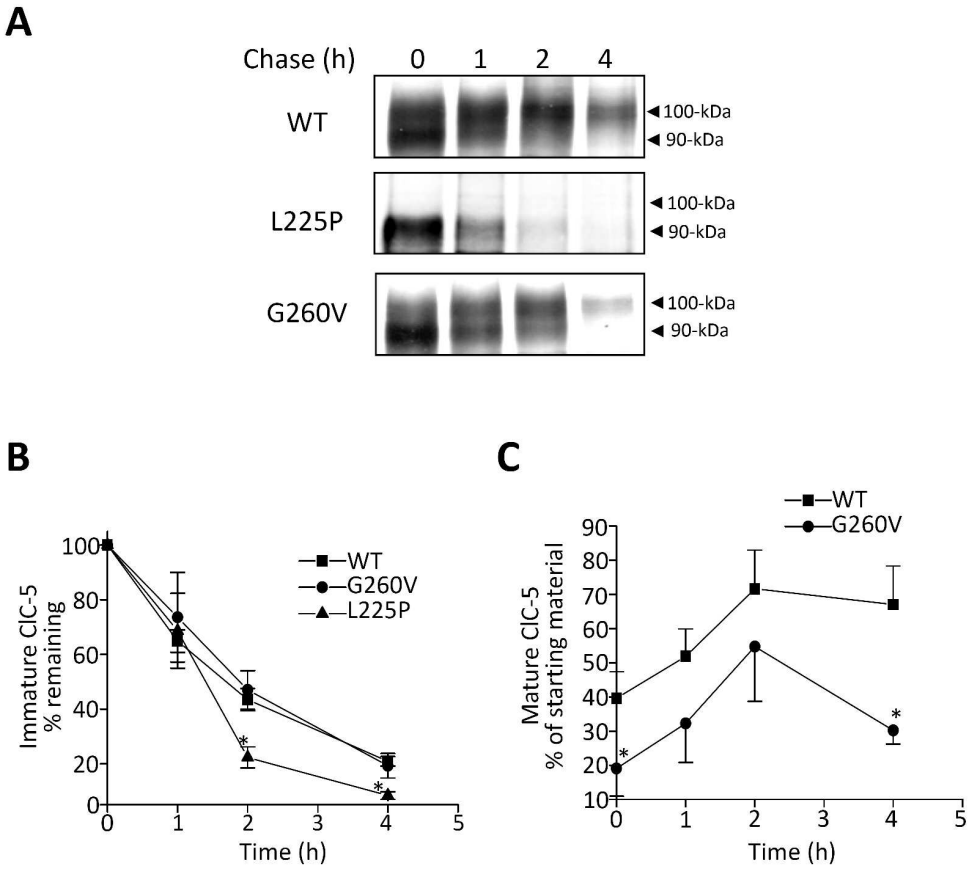

Figure 4

277x282mm (300 x 300 DPI)

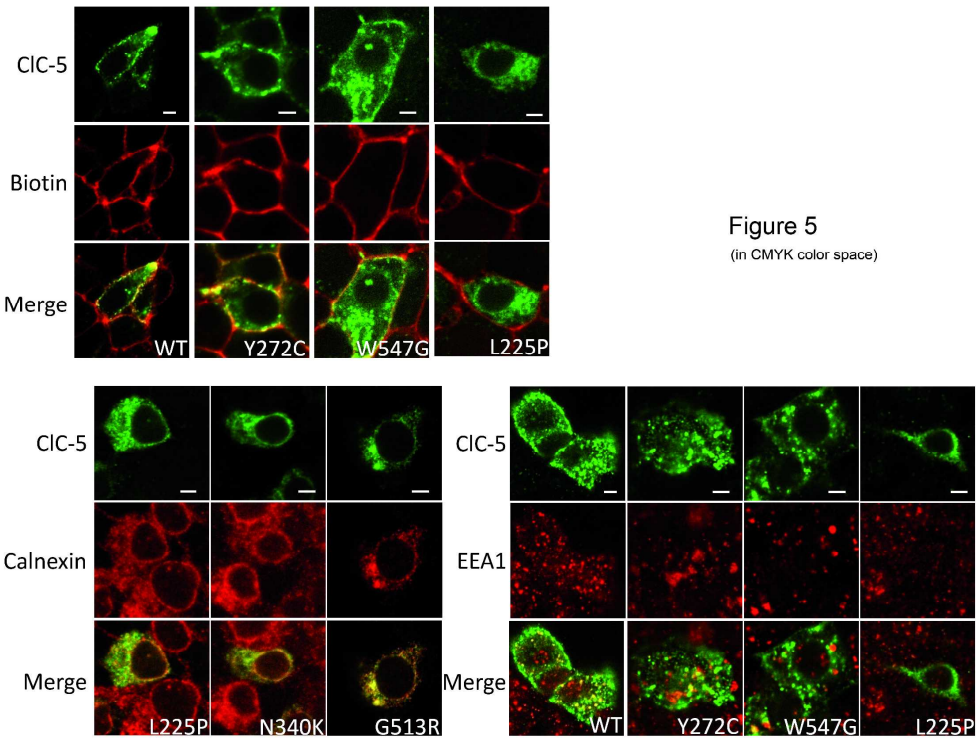

Figure 5
(in CMYK color space)

383x286mm (300 x 300 DPI)

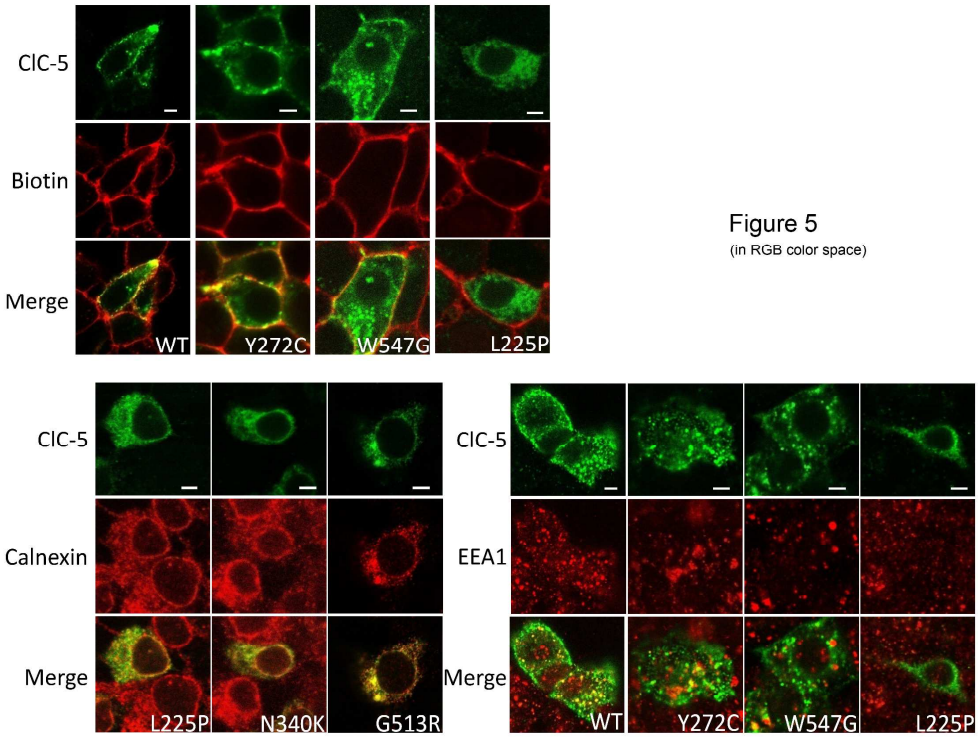

Figure 5
(in RGB color space)

384x287mm (300 x 300 DPI)

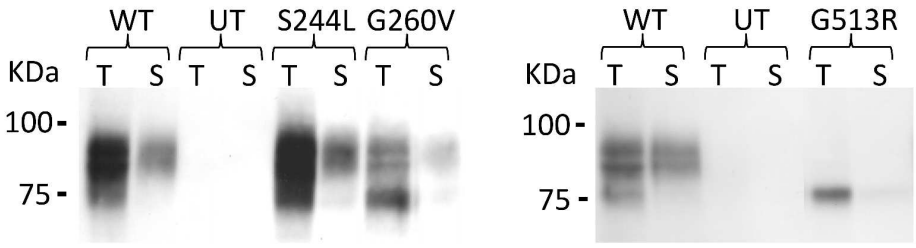

Figure 6

285x108mm (300 x 300 DPI)

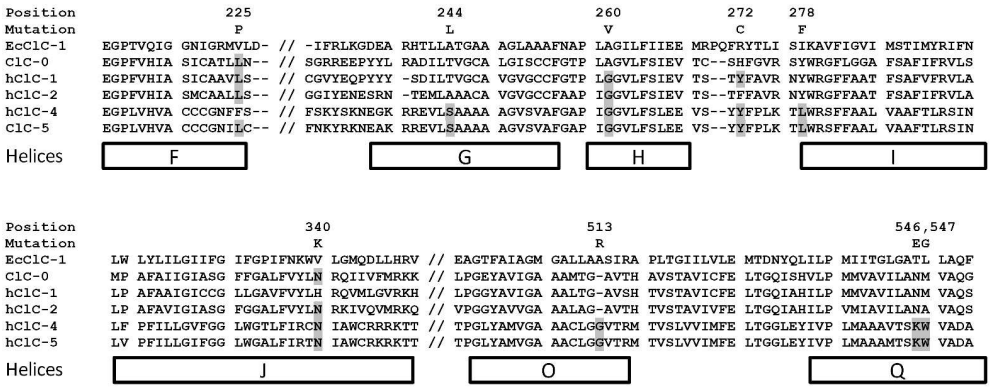

Figure 7

269x126mm (300 x 300 DPI)